Journal of ELECTRONIC MATERIALS, Vol. 39, No. 10, 2010
DOI: 10.1007/s11664-010-1333-y

Effect of Al-Trace Width on the Electromigration Failure Time of Flip-Chip Solder Joints

S.W. LIANG,[1] H.Y. HSIAO,[1] and CHIH CHEN[1,2]

1.—Department of Materials Science and Engineering, National Chiao Tung University, Hsin-chu 30010, Taiwan, ROC. 2.—e-mail: chih@cc.nctu.edu.tw

The effect of Al-trace width on electromigration (EM) in flip-chip solder joints was investigated experimentally. EM tests were performed on eutectic Sn-Ag solders with 40-μm- and 100-μm-wide Al traces. Under the same stressing conditions (0.5 A at 165°C), the failure time was 44.1 h for solder joints with 40-μm-wide traces and 250.1 h for solder joints with 100-μm-wide traces. The Al-trace width influenced both the current crowding and the Joule heating effects. Thus, both effects are responsible for the significant difference in failure time. Finite-element analysis was used to examine the current crowding effect in solder bumps with Al traces of the two different widths. The results showed that the current crowding effect was slightly higher in joints with 40-μm-wide traces. In addition, the temperature coefficient was used to measure the real temperatures in the solder bumps during EM. The results indicated that the width of the Al traces had a substantial influence on the Joule heating effect. The measured temperature in the solder bump was 218.2°C and 172.2°C for the bump with 40-μm- and 100-μm-wide Al traces, respectively. This difference in the Joule heating effect plays a crucial role in causing the difference in the failure time of solder joints with the two different widths.

Key words: Electromigration, electronic packaging

INTRODUCTION

Flip-chip technology has been used to package high-performance devices due to its high input/output density. Thousands of solder bumps are fabricated for a chip. Each solder bump is expected to carry 0.2 A. This value will be increased to 0.4 A in the future.[1] As portable products become smaller, the size of solder bumps must be scaled down. For these two reasons, the current density in the solder bump continues to increase, making electromigration (EM) a critical reliability issue for solder joints.[2] The line-to-bump geometry of flip-chip solder joints causes a serious current crowding effect in the solder bump near the entrance of the Al trace.[3,4] In addition, Al traces serve as the main heating source in flip-chip solder joints during accelerated EM tests.[5,6] The resistance of the Al trace ranges from several hundred to several thousand milliohms, depending on its dimensions. The resistance of the Al trace is about two orders of magnitude larger than the bump resistance. The heating power equation is expressed as follows:

$$P = I^2R, \tag{1}$$

where P is the Joule heating power, I is the current, and R is the resistance. The product I^2R is the total heating power. Because the resistance of the Al trace dominates the resistance of the stressing circuit, it plays a crucial role in the Joule heating effect in solder bumps.

To estimate the mean time to failure (MTTF) of joints, Black's equation is generally employed[7]:

$$\mathrm{MTTF} = A\frac{1}{j^n}\exp\left(\frac{Q}{kT}\right), \tag{2}$$

where A is a constant, j is the current density, n is a model parameter for the current density, Q is the

(Received July 26, 2009; accepted July 10, 2010; published online August 11, 2010)

activation energy, k is the Boltzmann constant, and T is the average bump temperature. This equation is suitable for Al and Cu interconnects. In view of the serious Joule heating and current crowding effect in solder joints, Choi et al.[8] proposed to modify the equation as follows:

$$\mathrm{MTTF} = A\frac{1}{(cj)^n}\exp\left[\frac{Q}{k(T+\Delta T)}\right]. \quad (3)$$

They proposed that the term j^{-n} in the equation must be revised as $(cj)^{-n}$ to include the current crowding effect in the solder joints. In addition, the temperature factor is modified as $(T + \Delta T)$ to account for the considerable Joule heating effect during accelerated EM tests.

Chiu et al.[9] investigated the effect of the length of an Al trace on EM lifetime. They found that the length of the Al trace affected the Joule heating effect, and the current crowding effect remained the same for solder joints with Al traces of various lengths. They also report that the length of the Al trace had a significant influence on the EM failure time of solder joints. Liang et al.[6] investigated the effect of the dimension of an Al trace on Joule heating and current crowding effects in solder bumps under EM using finite-element simulation. They reported that the width of the Al trace affected both the Joule heating and the current crowding effects. They predicted that a narrower Al trace would produce higher Joule heating and larger current crowding effects than a wider Al trace. Thus, trace width has a substantial effect on the failure time of solder joints. Al traces of different widths are commonly used in the packaging industry. However, this effect has not been verified by experimental results. In this study, we investigated EM failure in Sn-3.5Ag solder joints with 40-μm- and 100-μm-wide Al traces. The current crowding effect was calculated using simulations. In addition, the temperature coefficient of resistivity (TCR) effect was employed as a temperature sensor to measure the real temperature under current stressing. This approach helped to distinguish the Joule heating effect from the current crowding effect on the EM lifetime.

EXPERIMENTAL PROCEDURES AND SIMULATION

Lead-free Sn-3.5Ag solder joints were adopted, and the under-bump metallization (UBM) was 0.5 μm Ti-Cu/5 μm Cu. The dimensions of the solder joint are shown schematically in Fig. 1a. The 0.5 μm Ti-Cu was sputtered as a Cu seed layer, and then a 5 μm Cu layer was electroplated. The diameter of the UBM opening was 120 μm. Lead-free Sn-3.5Ag solder bumps were electroplated and joined to FR5 substrates. The bump height was about 75 μm. The metallization layer on the FR5 substrate was 5 μm electroless Ni. The Cu pad opening in the substrate was 300 μm in diameter. A daisy-chain structure with six bumps was adopted for the EM tests. Figure 1b illustrates the schematic layout of the testing structure. The pitch of the bumps was 850 μm.

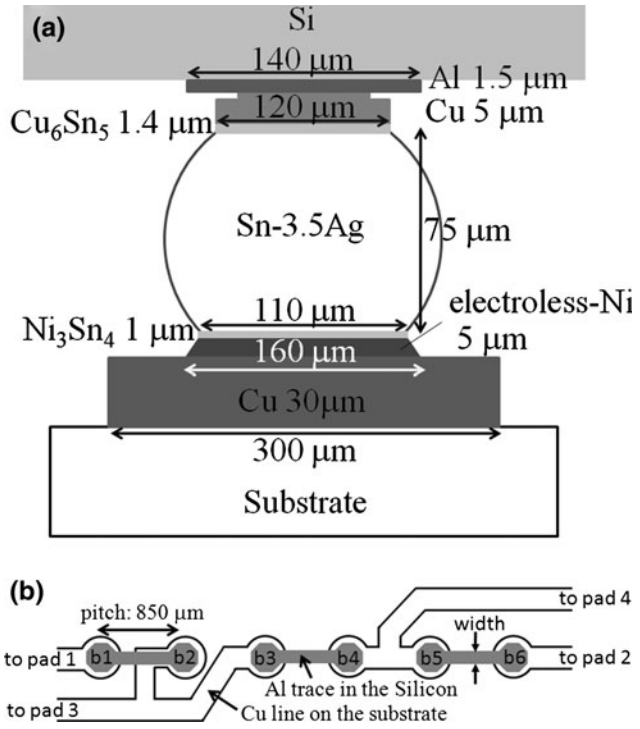

Fig. 1. (a) Schematic of the flip-chip solder joints adopted in this study. (b) Plan-view schematic showing the daisy-chain layout of the joints.

Table I. Properties of the materials used in the simulation models

Materials	Resistivity at 20°C ($\mu\Omega$ cm)
Al	3.2
Cu	1.7
Cu_6Sn_5	17.5
Sn-3.5Ag	12.3
Ni_3Sn_4	28.5
Electroless Ni	70.0

To investigate the effect of the width of the Al trace on EM, two test structures were adopted. The only difference between the two structures was the width of the Al traces; one trace was 40 μm wide, and the other was 100 μm wide. They were both 1.5 μm thick. During the EM tests, a current of 0.5 A was applied through pad 1 to pad 2 in Fig. 1b on a 165°C hot plate. The MTTF for each structure was obtained for five samples using the Weibull distribution. The resistance history was monitored using the four-point probe method at the Cu pads on the substrate side. The current was terminated by a computer program when the resistance of the stressing circuit exceeded 5×10^6 mΩ. An infrared

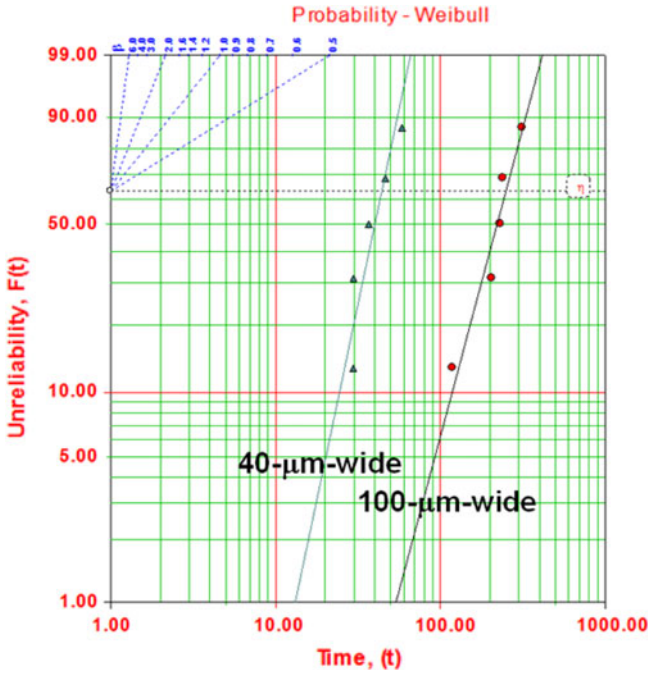

Fig. 2. Weibull distribution of the EM failure of the flip-chip solder joints with 40-μm- and 100-μm-wide Al traces.

Table II. Parameters determined from the Weibull plot

Width of Al Trace (μm)	β (Slope)	η (MTTF) (h)	ρ (Correlation) (%)
40	3.8	44.1	92.5
100	3.0	250.1	96.7

microscope was utilized to examine whether any damage occurred in the Al trace, because Si is transparent to infrared. After being checked by the infrared microscope, the samples were ground laterally with SiC papers and polished using Al_2O_3 powders. Scanning electron microscopy (SEM) was used to inspect the microstructure of the solder joints.

To examine the current-density distribution in the solder joints with Al traces of the two different widths, three-dimensional finite-element simulations were performed. Simulation models were constructed for the joints with 40-μm- and 100-μm-wide Al traces. The intermetallic compound (IMC) that formed between the UBM and the solder was also considered in the simulation models. The 0.5 μm of electroplated Cu was assumed to have been consumed to form a 1.4 μm layer of Cu_6Sn_5 IMC. Similarly, 0.5 μm of electroless Ni was assumed to react with the solder to form 1.0 μm of

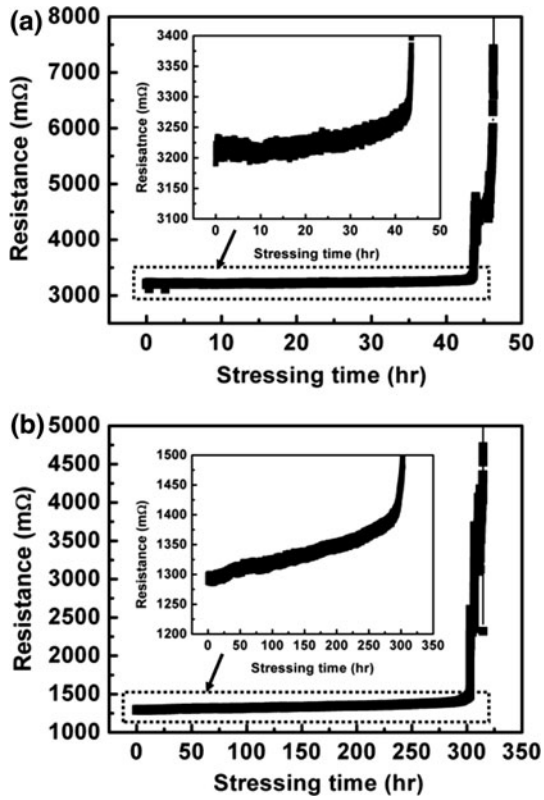

Fig. 3. (a) Changes in the resistance of the six solder joints with 40-μm-wide Al traces during EM tests. (b) Changes in the resistance of the six solder joints with 100-μm-wide Al traces during the EM tests. The *insets* show enlargements of the resistance curve for up to 95% of failure time.

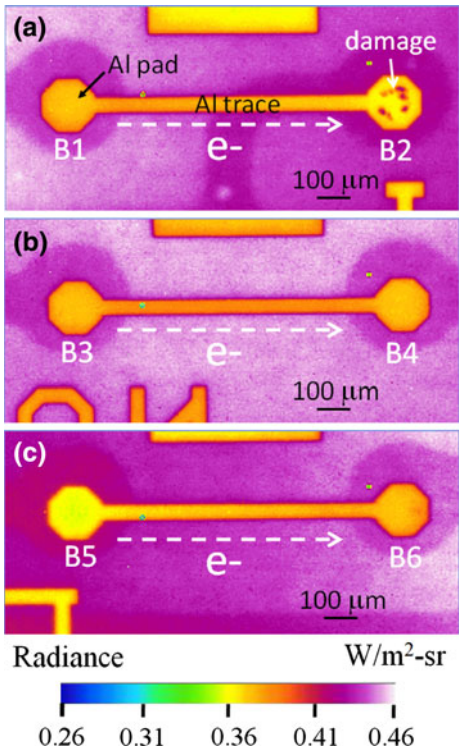

Fig. 4. (Color online) Plan-view radiance-mode infrared (IR) images for the 40-μm-wide Al traces after 0.5 A current stressing at 165°C. (a) First segment of the Al trace. Serious damage is present in the Al pad of bump 2. (b) Second segment of the Al trace. (c) Third segment of the Al trace.

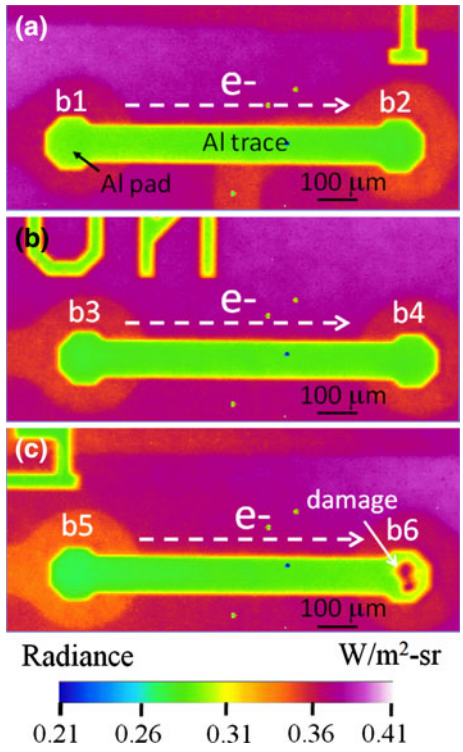

Fig. 5. (Color online) Plan-view radiance-mode IR images for the 100-μm-wide Al traces after 0.5 A current stressing at 165°C. (a) First segment of the Al trace. (b) Second segment of the Al trace. (c) Third segment of the Al trace. Serious damage is present in the Al pad for bump 6.

Ni_3Sn_4 IMC. Layer-type IMCs were used in this simulation for both the Cu_6Sn_5 and Ni_3Sn_4 layers to avoid meshing difficulty. The parameters of the materials used in this simulation are listed in Table I. The model used in this study involves the use of SOLID69 eight-node hexahedral coupled-field elements and ANSYS simulation software (ANSYS Inc., USA).

To measure the temperature in the solder bump, we took advantage of the TCR effect of the stressing circuit. The layout of this circuit is shown in Fig. 1b. For TCR calibration, a current of 0.2 A was applied from pad 1 to pad 2 in an oven, and the voltage drop through pad 3 and pad 4 was monitored. Thus, the measured resistance included the resistance of bump 3 and bump 4, some Cu lines, and the resistance of the Al trace connecting bump 3 and bump 4. To calibrate the TCR, the resistance was measured in an oven ranging from 50°C to 175°C. Thus, the real bump temperature was estimated when the bumps were stressed with 0.5 A on the 165°C hotplate.

RESULTS

The experimental results indicate that the width of the Al trace significantly influences the failure time of the solder joints. Figure 2 shows that the MTTFs of the solder joints with 40-μm- and 100-μm-wide Al traces were 44.1 h and 250.1 h, respectively. Other parameters determined from the Weibull plot are listed in Table II. The resistance histories of the two sets of joints show similar behavior under current stressing. Figure 3a and b illustrates typical resistance curves for the solder joints with 40-μm- and 100-μm-wide Al traces, respectively. The initial resistance was 3210.8 mΩ and 1292.9 mΩ for the joints with 40-μm- and 100-μm-wide Al traces, respectively. The resistance included the resistance of six bumps, three segments of Al trace, and the Cu lines in the substrate. Thus, the total resistance was higher for the joints with 40-μm-wide Al traces. The resistance increased slowly and almost linearly before 95% of the failure time, as shown in the insets to Fig. 3a and b. After this increase, the resistance increased abruptly until open-circuit failure occurred.

After EM failure, infrared microscopy was employed to examine whether damage occurred in the Al traces. Figure 4a–c shows plan-view radiance images for the solder joints with 40-μm-wide Al traces. The six bumps were situated directly below the six Al pads. The electron flow in the Al traces drifted from the left-hand side to the right-hand side. As seen in Fig. 4a, some damage occurred in the Al pad of bump 2, whereas no obvious damage was found in the Al traces connecting the bumps. However, in other samples, we found damage in the

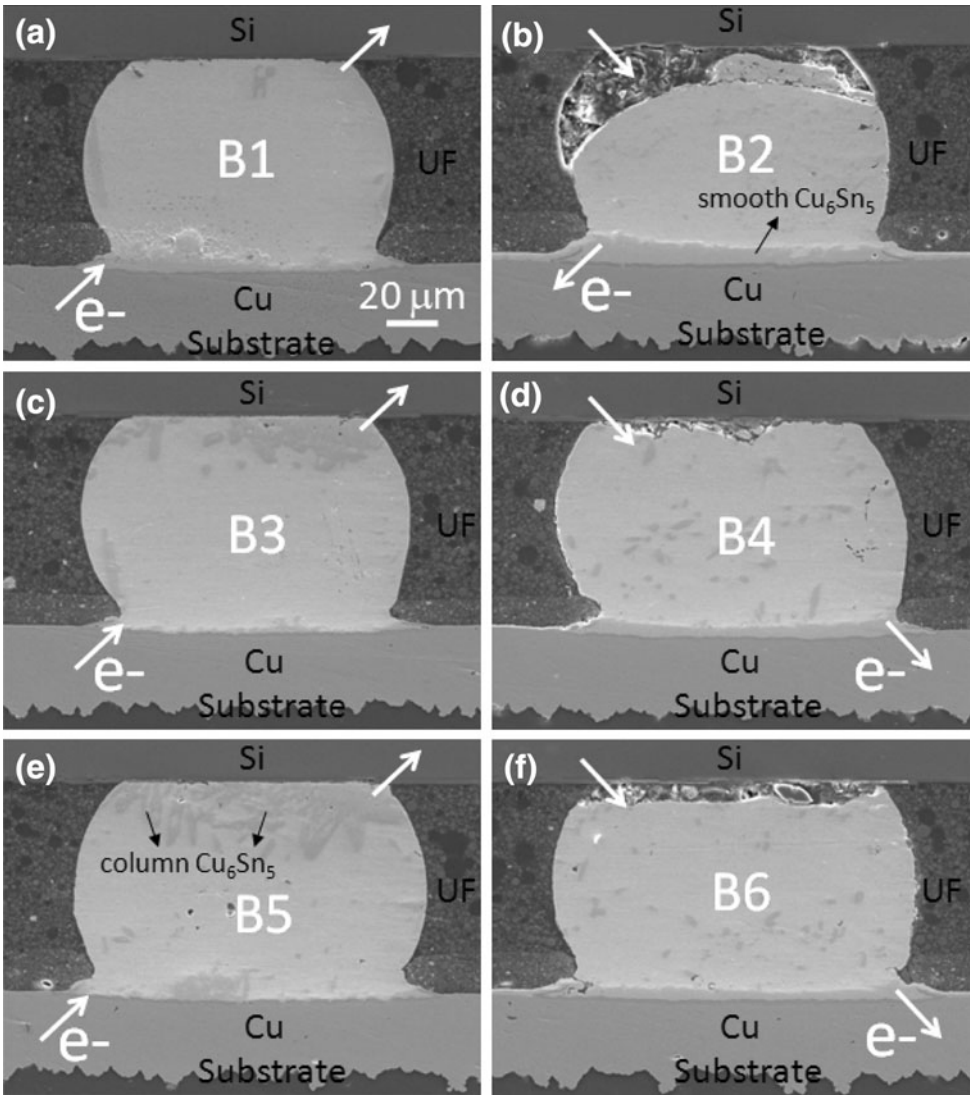

Fig. 6. Cross-sectional SEM images for the six bumps with 40-μm-wide Al traces after 0.5 A current stressing at 165°C. (a) Bump 1 with upward electron flow. (b) Bump 2 with downward electron flow. Large voids were found on the chip side. (c) Bump 3 with upward electron flow. (d) Bump 4 with downward electron flow. (e) Bump 5 with upward electron flow. (f) Bump 6 with downward electron flow.

Al pads of bump 4 or bump 6, because electrons drifted from the chip side to the substrate side for the even-numbered bumps. Serious damage always occurred in the Al pads of even-numbered bumps in this study. Similar failure modes were found in the Al pads for the solder joints with 100-μm-wide Al traces (Fig. 5). Serious damage was observed in the Al pad of bump 6.

To observe the failure sites in more detail, the samples were ground and polished laterally for cross-sectional SEM examination. Figures 6 and 7 show cross-sectional SEM images of the solder joints with 40-μm- and 100-μm-wide Al traces, respectively; the arrows indicate the direction of electron flow. For solder joints with 40-μm-wide Al traces, bump 2 had severe damage and almost opened. This result is consistent with the results of the infrared microscopy in Fig. 4. For solder joints with 100-μm-wide Al traces, bump 6 had the most serious damage of all the bumps. This result is also consistent with the infrared results in Fig. 5. All bumps with electrons drifting down had void formation on the chip side. In addition, the SEM results show that the IMC accumulated on the anode side due to the electron flow. When the electron current in the bump drifted downward (from the chip side to the board side), a smooth Cu_6Sn_5 layer accumulated on the anode side on the Cu pad due to the polarity effect.[10] Moreover, substantial column-type Cu_6Sn_5 accumulated in the anode on the chip side, especially close to the current crowding region. The supply of Cu atoms came from the Cu pad on the substrate side. Huang et al.[11] reported that Cu that migrates in the molten solder under current stressing produces substantial column-type Cu_6Sn_5. Similar behavior was found in this study. The solder

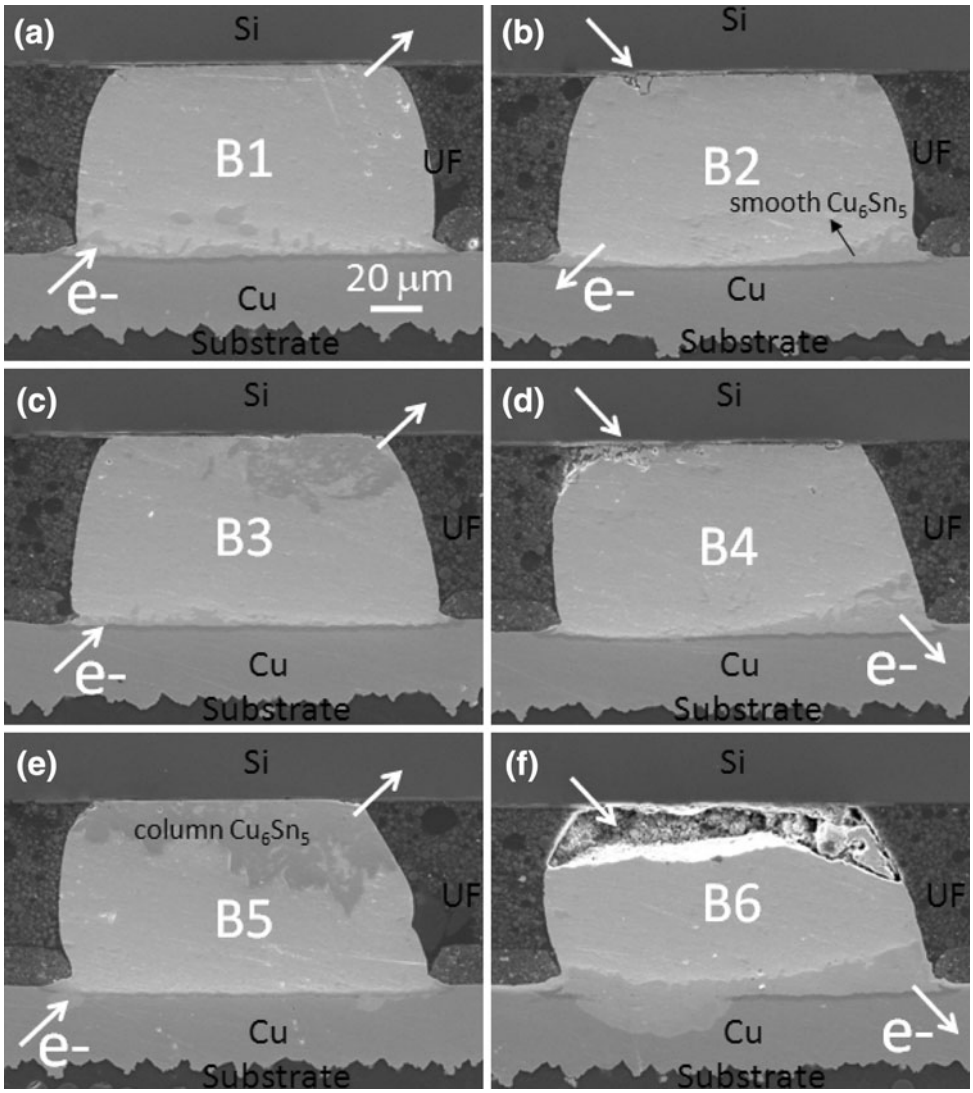

Fig. 7. Cross-sectional SEM images for the six bumps with 100-μm-wide Al traces after 0.5 A current stressing at 165°C. (a) Bump 1 with upward electron flow. (b) Bump 2 with downward electron flow. (c) Bump 3 with upward electron flow. (d) Bump 4 with downward electron flow. (e) Bump 5 with upward electron flow. (f) Bump 6 with downward electron flow. This bump has the most severe damage of the six bumps.

melted during the final 5% of the stressing time. Abundant Cu atoms migrated in the melted solder joints. No serious column-type Cu_6Sn_5 formed in the solder joints with downward electron current, for two possible reasons. First, the 5 μm Cu UBM on the chip side was totally consumed before solder melting, and insufficient Cu atoms were present to migrate to the board side to form the IMCs. Second, the temperature on the substrate side was lower than the temperature on the chip side. In our previous study, the damaged Al trace induced a high Joule heating effect and melted the eutectic Sn-Pb solder joints.[12] Because eutectic Sn-Ag was adopted in this study, it would only melt locally, due to its higher melting point. Serious column-type Cu_6Sn_5 was formed near the current crowding region with higher temperature.[13] Therefore, the IMCs formed at the anode/chip and anode/substrate ends of the solder joints have two different morphologies.

DISCUSSION

To distinguish between the current crowding effect and the Joule heating effect on failure time, the maximum current density and temperature in the solder joints must be obtained. First, the maximum current densities in the solder bumps with Al traces of the two widths were simulated by the finite-element method. Detailed information on the simulation can be found in our previous study.[6] Figure 8a and b shows cross-sectional views of the current density distribution in the solder joints with 40-μm- and 100-μm-wide Al traces, respectively. The current crowding effect occurred in the solder near the entrance point of the Al trace. The maximum current density in the solder bump with a 40-μm-wide Al trace was 2.22×10^4 A/cm^2. The crowding ratio is denoted as the maximum value divided by the average current density on the UBM

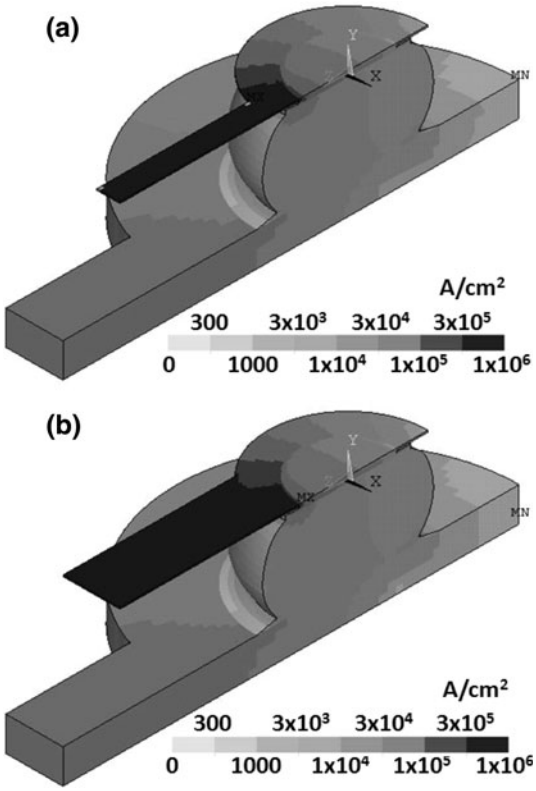

Fig. 8. Tilted cross-sectional views of the current-density distribution in the solder bump (a) with 40-μm-wide Al traces and (b) with 100-μm-wide Al traces when they were stressed by 0.5 A.

opening, which was 4.42×10^3 A/cm^2. The corresponding crowding ratio for the solder with a 40-μm-wide Al trace was 5.0. For the solder bump with a 100-μm-wide Al trace, the maximum current density decreased to 1.79×10^4 A/cm^2. Thus, increasing the width of the Al trace reduces the maximum current density in the solder bumps because a wider Al trace results in a lower average current density in the Al trace. Thus, the current density was smaller before going into the contact opening, leading to a smaller current density in the solder bump.

To measure the real temperature of the solder bumps during current stressing, the TCR effect of the stressing circuit was used as a temperature sensor in the package. Figure 9 shows the measured resistance as a function of oven temperature for the two widths. The measured resistance included a segment of the Al trace, two solder bumps, and some Cu lines in the substrate. However, most of the resistance came from the Al trace due to its small cross-section. Thus, the TCR effect originated mainly from the Al traces. Because the Al traces were connected to the solder bumps, the real temperature in the solder bumps was close to the temperature in the Al trace. The 0.2 A current was chosen because Joule heating under this current was less than 2°C, as measured by infrared

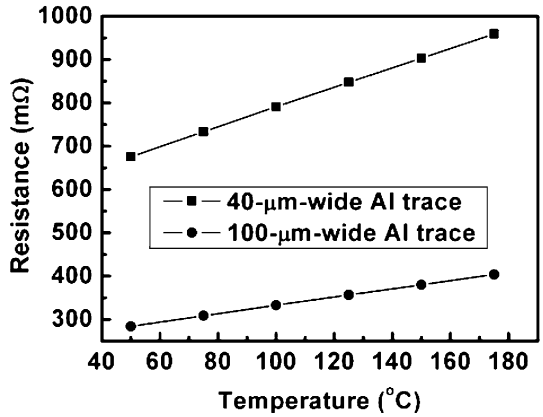

Fig. 9. Changes in the resistance as a function of oven temperature for solder joints with 40 μm-wide and with 100 μm-wide Al traces.

microscopy. The fitting equations for the two curves in Fig. 9 are

$$R_{40} = 563.0 + 2.27T \quad (4)$$

$$R_{100} = 236.5 + 0.96T, \quad (5)$$

where T is the real solder temperature, and R_{40} and R_{100} represent the resistance of the stressing circuit with 40-μm-wide and 100-μm-wide Al traces, respectively.

By using the fitting equations, the real temperature in the solder bumps was measured when a current of 0.5 A was applied to a circuit on a 165°C hotplate. The resistances were 1058.2 mΩ and 401.3 mΩ for the solder bumps with 40-μm- and 100-μm-wide Al traces, respectively. Thus, the real temperatures in the solders were estimated to be 218.2°C and 172.2°C for the solder bumps with 40-μm- and 100-μm-wide Al traces, respectively.

The different current crowding and Joule heating effects on the failure time were estimated using Black's equation. We used the simulated maximum current density as j and the measured temperature as T in Black's equation. The values of n and the activation energy were set at 2 and 0.7 eV, respectively. The estimated MTTF ratio of the solder joints with 100-μm-wide Al traces to those with 40-μm-wide Al traces was about 8.2. The current-density difference contributed 1.5-fold to the increase in MTTF, and the temperature variation contributed 5.5-fold to the increase in MTTF. The experimental MTTF ratio was about 5.7. Thus, a high Joule heating effect is the major reason for the short failure time of the solder joints with 40-μm-wide Al traces in this study. The temperature increase in the solder bump with 100-μm-wide Al traces was 46°C lower than that in the bumps with 40-μm-wide Al traces. Because of the exponential term in Black's equation, the increase in temperature has a pronounced influence on the MTTF of solder joints.

The difference in the current crowding effect has no substantial influence on the MTTF of bumps in the present case. However, if a thin-film UBM structure were adopted for the joints, the different current crowding effect may strongly influence the MTTF of joints.[6]

CONCLUSIONS

The effect of Al-trace width on EM in flip-chip solder joints was investigated experimentally. For the same stressing conditions (0.5 A on a 165°C hotplate), solder joints with larger trace widths had longer EM lifetime. The average failure time was 44.1 h and 250.1 h for solder joints with 40-μm- and 100-μm-wide Al traces, respectively. Different current crowding and Joule heating effects contributed to the difference in failure time. As described by Black's equation, these two factors affect the lifetime of the solder joint. According to the simulation results, a slightly higher current crowding effect occurs in solder joints with a 40-μm-wide Al trace than in joints with a 100-μm-wide Al trace. In addition, a higher Joule heating effect occurs for joints with a 40-μm-wide Al trace due to the larger resistance of the stressing circuit. By using the TCR effect of the stressing circuit, we obtained the real temperature in the solder joints. The different Joule heating effects were the main contributors to the different failure times for solder joints with Al traces of different widths.

ACKNOWLEDGEMENTS

The authors would like to thank the National Science Council of ROC for financial support through Grant No. 95-2221-E-009-088-MY3.

REFERENCES

1. K.N. Tu, *J. Appl. Phys.* 94, 5451 (2003).
2. K.N. Tu, *Solder Joint Technology* (New York: Springer, 2007).
3. E.C.C. Yeh, W.J. Choi, and K.N. Tu, *Appl. Phys. Lett.* 80, 4 (2002).
4. T.L. Shao, S.W. Liang, T.C. Lin, and C. Chen, *J. Appl. Phys.* 98, 044509 (2005).
5. S.H. Chiu, T.L. Shao, C. Chen, D.J. Yao, and C.Y. Hsu, *Appl. Phys. Lett.* 88, 022110 (2006).
6. S.W. Liang, Y.W. Chang, and C. Chen, *Appl. Phys. Lett.* 88, 172108 (2006).
7. J.R. Black, *IEEE Trans. Electron. Dev.* 16, 338 (1969).
8. W.J. Choi, E.C.C. Yeh, and K.N. Tu, *J. Appl. Phys.* 94, 5665 (2003).
9. S.H. Chiu, C. Chen, and D.J. Yao, *J. Electron. Mater.* 35, 1740–1744 (2006).
10. H. Gan and K.N. Tu, *J. Appl. Phys.* 97, 063514 (2005).
11. J.R. Huang, C.M. Tsai, Y.W. Lin, and C.R. Kao, *J. Mater. Res.* 23, 250 (2008).
12. S.W. Liang, S.H. Chiu, and C. Chen, *Appl. Phys. Lett.* 90, 082103 (2007).
13. H.Y. Hsiao, S.W. Liang, M.F. Ku, C. Chen, and D.J. Yao, *J. Appl. Phys.* 104, 033708 (2008).